Extended Abstracts of the 2015 International Conference on Solid State Devices and Materials, Sapporo, 2015, pp1102-1103

Formation of n^+Poly-Ge Films with High Electron Concentration and High Electron Mobility by Flash Lamp Annealing for Poly-Ge *n*MOSFETs

Masahiro Koike,[1,3] Koji Usuda,[1,3] Takahiro Mori,[1,2] Tatsuro Maeda,[1,2] and Tsutomu Tezuka[1,3]
[1] *Collaborative Research Team Green Nanoelectronics Center (GNC), National Institute of Advanced Industrial Science and Technology,*
[2] *National Institute of Advanced Industrial Science and Technology,*
[3] *Corporate Research and Development Center, Toshiba Corporation, 1, Komukai Toshiba-cho, Saiwai-ku, Kawasaki, 212-8582, Japan*
Phone: +81-44-549-2314 Fax: +81-44-520-1257 m-koike@mail.rdc.toshiba.co.jp

Abstract

n^+poly-Ge films were fabricated from amorphous Ge with various doses of P-ion implantation by annealing sequences using combinations of flash lamp annealing (FLA) and conventional furnace annealing (FA). It was clarified that crystallization by FA resulted in p^+poly-Ge films with high hole concentration (~10^{18} cm^{-3}) originating from acceptor-like defects; on the other hand, activation annealing by FLA resulted in n^+poly-Ge films with high electron concentration (~10^{19} cm^{-3}). Activation ratios as high as those for crystalline Ge and high electron mobility (>140 cm^2/Vs) exceeding the values for crystalline Si were achieved. The origin of these high values in the FLA-activated poly-Ge could be explained by the lower concentration of acceptor-like defects inside grain rather than the larger grain size compared to that in FA-activated poly-Ge.

1. Introduction

Poly-Ge is an attractive material for sequentially stacked 3D-integrated complementary metal oxide semiconductor (CMOS) circuits [1-3]. The lower process temperature compared to that for conventional Si CMOS is desirable for formation on the lower CMOS layer, preventing electrical degradation; however, the difficulty forming *n*-type poly-Ge must be resolved, since defects, such as vacancies, in Ge behave as acceptor-like defects, which generate holes; therefore, poly-Ge usually shows *p*-type characteristics with high hole concentration (~10^{18} cm^{-3}).

We previously reported n^+poly-Ge with high concentration and high mobility as well as p^+poly-Ge, using two-step flash lamp annealing (FLA), i.e., FLA before and after P-ion implantation (P-I/I) into Ge [1]. Tri-gate junctionless *n*- and *p*-MOSFETs with the n^+ and p^+poly-Ge exhibited high drive currents of 119 and 311 μA/μm, respectively; however, it was not clarified whether two-step FLA was more effective than FLA alone or different annealing methods such as furnace annealing (FA).

In the present study, we fabricated poly-Ge with various P-ion doses using different annealing methods, i.e., FLA, FA, and their combinations, and clarified that a sequence including final annealing by FLA was more effective in forming n^+poly-Ge with higher electron concentration and higher electron mobility.

2. Experiment

Poly-Ge films were formed and examined as follows [Fig. 1(a)]: amorphous Ge (a-Ge) films (~100 nm) were deposited by sputtering on thermal SiO_2 film (~200 nm)/Si substrates. P-I/I was used to change the carrier type from *p*-type to *n*-type, applying doses of 5×10^{14}, 1×10^{15}, 5×10^{15}, and 1×10^{16} cm^{-2}. FLA was 80 J/cm^2 for 10 ms, whereas FA was 500°C for 5 h. Four annealing sequences were employed to form poly-Ge films [Fig. 1(b)]: (i) P-I/I→FA (FA), (ii) FLA→P-I/I→FA (FLA-first), (iii) P-I/I→FLA (FLA-last), and (iv) FLA→P-I/I→FLA (two-step FLA). The structures were observed by plain and cross-sectional transmission electron microscopy (TEM). The profiles of P impurity concentration in poly-Ge were examined by secondary ion mass spectrometry (SIMS). Crystallographic orientation and grain size were investigated by electron backscatter diffractometry (EBSD). Carrier type, carrier concentration, and motility (Hall mobility) were estimated by Hall-effect analysis.

3. Results and Discussion

After the four annealing sequences [Fig. 1(b)], each a-Ge turned into poly-Ge, according to the cross-sectional TEM images (Fig. 2). Flat and continuous films were formed, and the thickness (~100 nm) remained almost unchanged after the annealing.

SIMS profiles of P in the poly-Ge showed that its diffusion depended on the initial annealing before P-I/I as well as the final annealing (Fig. 3). P diffused deeper into the poly-Ge films fabricated by FLA-first than by FA [Figs. 3(a) and 3(b)], suggesting that the crystallinity of the FLA-first poly-Ge was higher than that of the FA poly-Ge. P diffused to a greater extent and spread almost uniformly at a high dose ($\geq5\times10^{15}$ cm^{-2}) in poly-Ge films fabricated by FLA-last and two-step FLA [Figs. 3(c) and 3(d)]. This implies that P could diffuse inside the grains as well as the grain boundaries, probably because final annealing by FLA produced larger grains with higher crystallinity compared to final annealing by FA, leading to the reduction of grain boundaries and defects in grains. After the diffusion, a region, e.g., around the surface with P >10^{20} cm^{-3} existed, which would be high enough to compensate for the holes, if P in poly-Ge were sufficiently electrically activated.

The grain size of poly-Ge depended on the dose of P and the annealing sequence. A higher dose led to a larger grain size in two-step FLA poly-Ge, whereas it led to a smaller grain size in FLA-last poly-Ge (Fig. 4), even though the final annealing in both cases was FLA. The difference between the two suggests that poly-Ge was not completely melted by FLA and partially crystallized Ge, resulting from the initial annealing of FLA or FA, still remained. We consider that the partially crystallized Ge worked as a nucleus and that the difference in crystallinity before FLA caused the difference in grain size.

The shape of grains of the poly-Ge by FLA-last and by two-step FLA tended to grow with anisotropy, i.e., in a horizontal direction, whereas that of poly-Si by FA grew without anisotropy. The results of EBSD also showed the anisotropic growth of the poly-Ge (Fig. 5). This is probably because FLA caused a horizontal temperature gradient in the films, leading to the anisotropic growth.

Hall measurement revealed that an annealing sequence including FLA turned poly-Ge into *n*-type. FLA-first, FLA-last, and two-step FLA poly-Ge changed from *p*-type to *n*-type with increasing P dose (Fig. 6). In particular, FLA-last poly-Ge and two-step FLA poly-Ge reached a high electron concentration of 1×10^{19} cm^{-3}, and two-step FLA could turn poly-Ge into *n*-type at a P dose of 1×10^{15} cm^{-2}, lower than that by FLA-last. On the other hand, FA poly-Ge remained as a *p*-type even at a high dose of 1×10^{16} cm^{-2}. Undoped Poly-Ge films fabricated by FLA (FA) showed hole concentration of ~2×10^{18} (~8×10^{18}) cm^{-3}. It was suggested that FLA could result in poly-Ge films with higher crystallinity compared to FA. Since lower hole concentrations corresponded to the lower defect concentrations, FLA could possibly reduce defects and activate P in poly-Ge compared with FA.

The average electrical activation ratio of P was higher in poly-Ge films fabricated by annealing including FLA than that in poly-Ge films reported previously [fabricated by solid phase crystallization (SPC) and by metal induced crystallization (MIC)] [4] and was comparable to that in crystalline Ge [6] (Fig. 7). We consider that annealing sequences including FLA formed poly-Ge films with higher crystallinity as described above, resulting in a higher activation ratio.

Our poly-Ge films fabricated by FLA exhibited high electron mobility; in the case of final annealing by FLA, i.e., FLA-last and two-step FLA, electron mobility in each poly-Ge reached ~140 cm^2/Vs (Fig. 8).

Interestingly, the mobility seemed to have a low correlation to the grain size (Fig. 9), where the average grain size was estimated from EBSD images. Instead, the crystallinity was probably related to the mobility, since poly-Ge films fabricated using FLA exhibited a higher hole mobility compared to that fabricated using FA.

Mobility for the poly-Ge in this study was higher than that for the poly-Ge films fabricated by SPC and MIC in a previous study [4] and that for the crystalline Si (c-Si) [5]. Thus, final annealing with FLA was effective in forming n^+poly-Ge films with high electron concentration and high electron mobility.

4. Summary

n^+poly-Ge films were fabricated from sputter-deposited a-Ge with various doses of P-I/I (0.05–1×10^{16} cm^{-2}), using various annealing sequences including FLA. It was clarified that FA (500°C, 5 h) resulted in p^+poly-Ge films with high hole concentration (~10^{18} cm^{-3}), originating from acceptor-like defects; on the other hand, final annealing by FLA resulted in n^+poly-Ge films. High electron concentration (~10^{19} cm^{-3}) resulting from a high activation ratio comparable to that of c-Ge, and high electron mobility (>140 cm^2/Vs) exceeding the values for c-Si, were achieved. These high values had a low correlation to the grain size and could be explained by the low concentration of acceptor-like defects inside grains and high activation of P in poly-Ge films.

Acknowledgments

We thank the entire technical staff at AIST for supporting our experiment. This research was partially supported by a grant from JSPS through the FIRST Program initiated by CSTP.

References

[1] K. Usuda et al., IEDM Tech. Dig., 422 (2014).
[2] Y. Kamimuta et al., VLSI-TSA, 109 (2013).
[3] Y. Kamata et al., SSDM, 668 (2014).
[4] H. –W. Jung et al., J. Alloy and Compounds, **561**, 231 (2013).
[5] C. Jacoboni et al., Solid State Electron. **20**, 77 (1977).
[6] M. Koike et al., J. Appl. Phys. **104**, 023523 (2008).

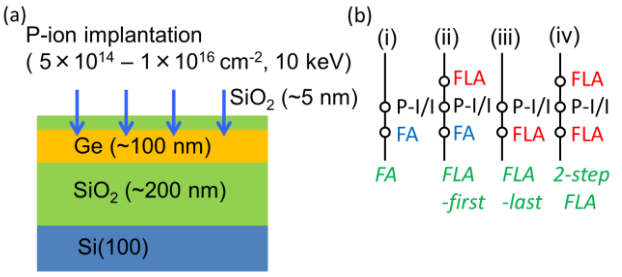

FIG. 1: Schematic of (a) sample structure and (b) annealing process in this study. Four annealing sequences were compared, where FA indicates furnace annealing (500°C, 5 h), and FLA indicates flash lamp annealing.

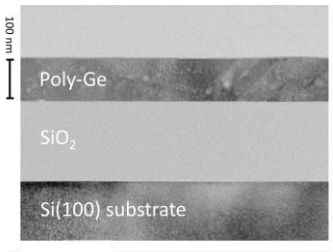

FIG. 2: Cross-sectional TEM image of poly-Ge fabricated by two-step FLA (Fig. 1). The dose of P-I/I was 1×10^{16} cm^{-2}.

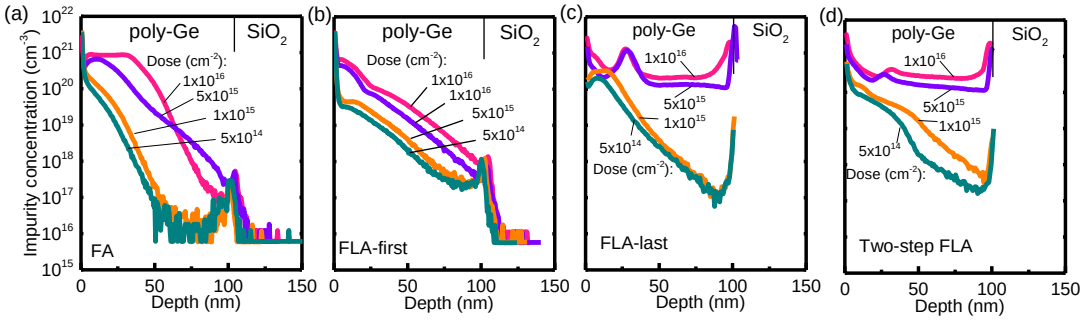

FIG. 3: Profiles of P in poly-Ge (Figs. 1 and 2) fabricated by four annealing sequences (Fig. 1): (a) FA, (b) FLA-first, (c) FLA-last, and (d) two-step FLA. The doses of P-I/I were 5×10^{14}, 1×10^{15}, 5×10^{15}, and 1×10^{16} cm^{-2}.

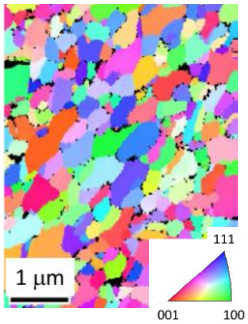

FIG. 5: EBSD image of poly-Ge fabricated by two-step FLA. The dose of P-I/I was 1×10^{16} cm^{-2}.

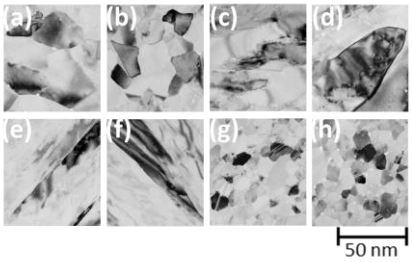

FIG. 4: Plain TEM images of poly-Ge fabricated by (a)-(d) two-step FLA and (e)-(h) FLA-last. The doses of P-I/I were (a),(e) 5×10^{14}, (b),(f) 1×10^{15}, (c),(g) 5×10^{15}, and (d),(h) 1×10^{16} cm^{-2}.

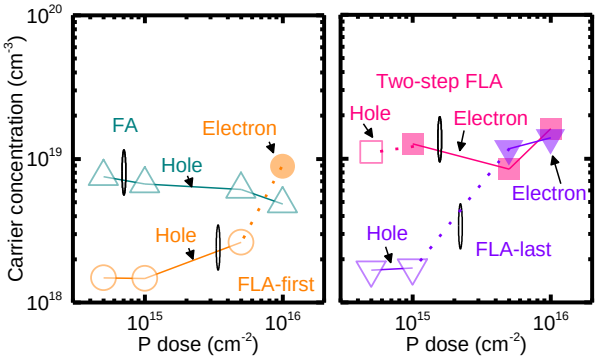

FIG. 6: Relationship between carrier concentration and P-I/I dose in poly-Ge. Open symbols indicates holes; closed symbols indicate electrons.

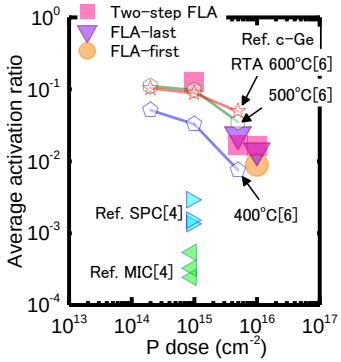

FIG. 7: Relationship between P-dose and average activation ratio. The data for poly-Ge by MIC and SPC [4] and for c-Ge [6] is also depicted.

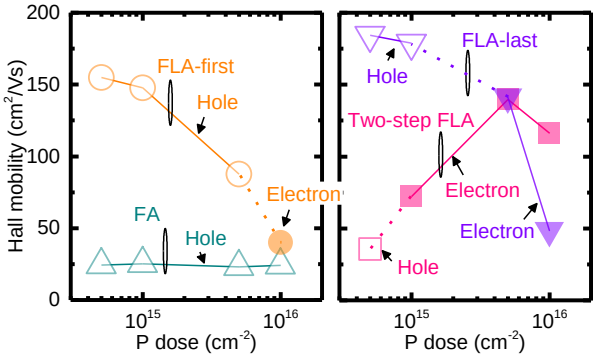

FIG. 8: Relationship between Hall mobility and P-I/I dose in poly-Ge. Open symbols indicate holes; closed symbols indicate electrons.

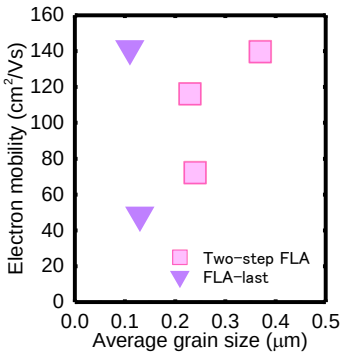

FIG. 9: Relationship between average grain size and electron mobility. Average grain size was estimated from EBSD images (Fig. 5).

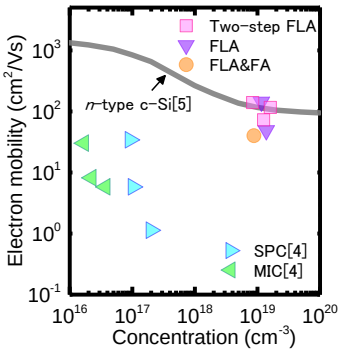

FIG. 10: Electron mobility of poly-Ge and crystalline Si. The data of Ref. (MIC) and Ref. (SPC) is from [4].